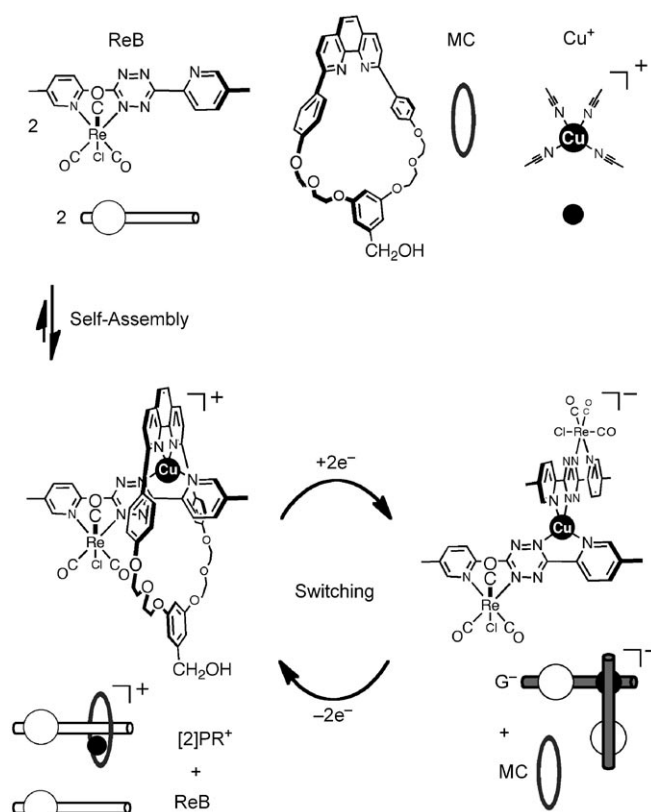


# Interconverting Two Classes of Architectures by Reduction of a Self-Sorting Mixture

Kumar Parimal, Edward H. Witlicki, and Amar H. Flood\*

Supramolecular complexity finds its ultimate expression in the structures and functions of natural systems. Chemists are emulating these properties individually in the form of self-assembling<sup>[1]</sup> complexes (e.g., squares,<sup>[2]</sup> polyhedra<sup>[3]</sup>) and molecular switches<sup>[4]</sup> (e.g., catenanes and rotaxanes<sup>[5]</sup>), respectively. Combinations of the two, that is, stimuli-responsive self-assembled complexes, are rare. Most self-assemblies will disassemble upon stimulation (e.g., pseudorotaxanes<sup>[6,7]</sup> and tetrahedra<sup>[8]</sup>). Other systems switch within the same architectural manifold (e.g., from one pseudorotaxane into another<sup>[9]</sup>). While the ability to transform between two different self-assembled architectures (pincer and grid,<sup>[10]</sup> ring and cage,<sup>[11]</sup> from 2D to 3D<sup>[12]</sup>) is growing in number, these demonstrations make use of chemical stimuli. Use of redox stimulation, with its macro-to-molecule interface and the ability to cycle many times, is unprecedented. Herein, we demonstrate this capability with the facile and reversible interconversion between two different architectures (Scheme 1) using electrons instead of chemicals.

We self-assembled different architectures around a dynamic  $\text{Cu}^{\text{I}}$  ion<sup>[13]</sup> and used ligand reduction<sup>[14]</sup> to switch between them. The ligand's steric, electrostatic, and electronic ( $\sigma/\pi$ ) properties can be used to direct which architecture is formed.<sup>[15]</sup> Two different ligands were designed to access two  $\text{Cu}^{\text{I}}$  complexes. The first ligand, ReB (Scheme 1), is based on a bischelating 3,6-bis(5-methyl-2-pyridyl)-1,2,4,5-tetrazine ( $\text{Me}_2\text{BPTZ}$ ) ligand system,<sup>[14]</sup> which reduces easily. The  $\text{Me}_2\text{BPTZ}$  ligand is mononucleated with the rhenium(I) tricarbonylchloro,  $[\text{Re}(\text{CO})_3\text{Cl}]$ , moiety to afford one chelating site, rather than two, thus simplifying the complexity of the self-sorting mixture (Scheme 1). The two nitrogen atoms that make up the open chelating site have very different electronic characters: The pyridyl N is a strong  $\sigma$  donor and weak  $\pi$  acceptor while the tetrazyl N is a weak  $\sigma$  donor and strong  $\pi$  acceptor.<sup>[16]</sup> Upon tetrazine-localized reduction of the ReB ligand,<sup>[17]</sup> the electronic properties of the tetrazine core invert (strong  $\sigma$  donor and  $\pi$  donor) while the pyridine unit will be relatively unchanged. The second ligand is a strong  $\sigma$ -donating, sterically bulky and redox-innocent phenanthroline-based macrocycle, MC (Scheme 1), which prevents the formation of a bis-macrocycle complex.<sup>[18]</sup>



**Scheme 1.** A self-sorting mixture of two ligands (ReB and MC) around a  $\text{Cu}^{\text{I}}$  ion shows redox-driven interconversion between two distinct architectures: pseudorotaxane,  $[2]\text{PR}^+$ , and grid-corner complex,  $\text{G}^-$ . (White and gray rods are neutral and reduced, respectively.)

Using ReB and MC as ligands, only two architectures can be formed in a mixture with  $\text{Cu}^{\text{I}}$  ions. The first is a heteroleptic complex wherein the ReB ligand is templated by the  $\text{Cu}^{\text{I}}$  ion to thread through the macrocycle to produce a  $[2]\text{pseudorotaxane}$ ,  $[2]\text{PR}^+$  (Scheme 1). The second involves two ReB ligands to form a homoleptic complex,  $\text{G}^+$ , which resembles a corner piece of grid-type complexes.<sup>[2,3]</sup> On electronic grounds the heteroleptic complex,  $[2]\text{PR}^+$ , is expected to be more stable: It has a total of three strong  $\sigma$ -donor nitrogen atoms and utilizes the strongly stabilizing macrocycle.<sup>[18]</sup> Upon ligand-based reduction of an appropriate mixture, the reduced form of the grid corner,  $\text{G}^-$  (Scheme 1), can be electrostatically stabilized<sup>[19]</sup> with the installation of two negative charges. In order to test these ideas, a mixture of the three components  $\text{Cu}^{\text{I}}:\text{ReB}:\text{MC}$  was prepared in the ratio 1:2:1 and the mechanism of switching between the two architectures was verified using digital

[\*] K. Parimal, E. H. Witlicki, Prof. A. H. Flood  
Chemistry Department, Indiana University  
800 East Kirkwood Avenue, Bloomington, IN 47405 (USA)  
Fax: (+1) 812-855-8300  
E-mail: aflood@indiana.edu  
Homepage: <http://www.indiana.edu/~floodweb/>

Supporting information for this article is available on the WWW under <http://dx.doi.org/10.1002/anie.201001003>.

simulations of the cyclic voltammetry (CV). Surprisingly, conversion was also initiated upon reduction of a single [ReB] ligand in [2]PR<sup>+</sup>, stemming from the ligand-based mixed valency<sup>[20]</sup> of G<sup>0</sup>.

Preparation of ligand ReB,<sup>[17]</sup> macrocycle MC,<sup>[14]</sup> and Cu<sup>I</sup> source, [Cu(MeCN)<sub>4</sub>]<sup>+</sup>PF<sub>6</sub><sup>−</sup>,<sup>[21]</sup> were reported previously. The identity of the two architectures, [2]PR<sup>+</sup> and G<sup>+</sup>, was confirmed by electrospray ionization mass spectrometry.<sup>[22]</sup> X-Ray crystallography of ReB confirmed the different coordination properties of the two nitrogen atoms. The pyridyl Re–N bond (2.189(5) Å) is longer than the tetrazyl Re–N bond (2.124(5) Å), consistent with a larger degree of Re–tetrazine back bonding.<sup>[23]</sup>

The self-assembly of [2]PR<sup>+</sup> and that of G<sup>+</sup> were investigated separately. The first of these involves the formation of [2]PR<sup>+</sup> (Figure 1a), with diagnostic UV/Vis/

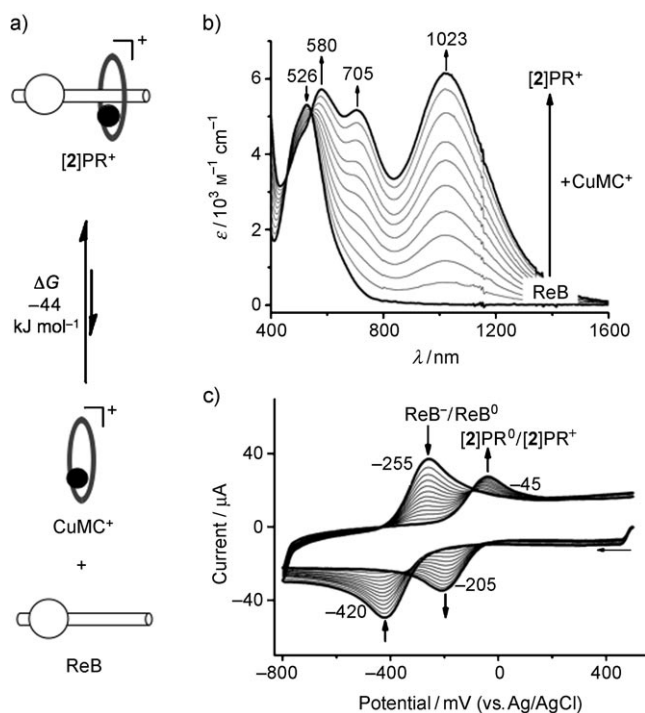


**Figure 1.** a) Self-assembly process for the formation of [2]PR<sup>+</sup>, observed by b) UV/Vis/NIR titration (50  $\mu\text{M}$ ,  $\text{CH}_2\text{Cl}_2$ , up to 1.0 equiv of CuMC<sup>+</sup>). c) Titration of CuMC<sup>+</sup> ( $\text{CH}_2\text{Cl}_2$ ) into ReB observed using CV ([ReB]<sub>0</sub> = 0.5 mM, up to 1.2 equiv of CuMC<sup>+</sup>, 0.1 M TBAPF<sub>6</sub>, 20 V s<sup>−1</sup>, glassy carbon, iR compensated).

NIR (Figure 1b) and IR<sup>[22]</sup> absorption spectra and CV responses (Figure 1c). The ligand, ReB, shows an absorption centered at 526 nm (= 2.4 eV) of medium intensity ( $\epsilon = 5200 \text{ M}^{-1} \text{ cm}^{-1}$ ) that was assigned<sup>[17]</sup> to a Re→Me<sub>2</sub>BPTZ metal-to-ligand charge-transfer (MLCT) transition on the basis of time-resolved IR spectroscopy. When the preformed copper macrocycle, CuMC<sup>+</sup> (Figure 1a), was titrated into a dilute solution of ReB three absorption bands are observed (Figure 1b) to grow in at 580, 705 and 1023 nm concomitant with the disappearance of the parent spectrum. The changes reached saturation at 1.0 equivalents of CuMC<sup>+</sup> and gener-

ated stable isosbestic points consistent with the quantitative formation of [2]PR<sup>+</sup> (Figure 1b). The low-energy band at 1023 nm (ca. 1.2 eV) is assigned to a Cu→Me<sub>2</sub>BPTZ MLCT transition: The small energy gap arises when the coordinated Cu<sup>I</sup> ion introduces an accessible HOMO and both electropositive centers (Re<sup>I</sup> and Cu<sup>I</sup>) stabilize the tetrazine-based LUMO. Equilibrium-restricted factor analysis<sup>[22,24]</sup> of the spectroscopic titration is consistent with a self-assembly formation energy of  $\Delta G = -44 \text{ kJ mol}^{-1}$  for [2]PR<sup>+</sup> when employing the known<sup>[14]</sup> formation energy for CuMC<sup>+</sup> ( $\Delta G = -29 \text{ kJ mol}^{-1}$ ).

CV titrations (Figure 1c) show the tetrazine-localized reduction of ReB to become easier upon formation of [2]PR<sup>+</sup>. The CVs were recorded at a fast scan rate (20 V s<sup>−1</sup>) in order to limit the amount of time available for any switching.<sup>[25]</sup> The ReB ligand displays one reduction<sup>[26,27]</sup> at  $E' = -350 \text{ mV}$  assigned to the tetrazine.<sup>[14,17]</sup> This process is stabilized by 625 mV compared to the parent Me<sub>2</sub>BPTZ ligand<sup>[14]</sup> and is consistent with the electropositive and strong  $\pi$ -acceptor properties of [Re(CO)<sub>3</sub>Cl].<sup>[23]</sup> Upon addition of CuMC<sup>+</sup> to form [2]PR<sup>+</sup> the Me<sub>2</sub>BPTZ-based reduction at −125 mV is stabilized by 225 mV and displays a 33% decrease in peak intensity, which is attributed to a concomitant decrease in the diffusion coefficient.<sup>[14]</sup> The Cu<sup>I</sup>/Cu<sup>II</sup> oxidation process<sup>[22,26]</sup> is observed at  $E' = +850 \text{ mV}$ . Consequently, the potential difference between the reduction and oxidation processes ( $\Delta E_{\text{redox}}$ ) decreases from approximately 2.0 eV for ReB<sup>[22]</sup> to 0.975 eV for [2]PR<sup>+</sup> consistent with the MLCT assignment of the UV/Vis/NIR absorption bands (Figure 1b).

The facial tricarbonyl groups on the rhenium(I) center allowed the influence of CuMC<sup>+</sup> coordination on the  $\pi$ -electron density of ReB to be investigated. Upon formation of [2]PR<sup>+</sup>, the carbonyl bands shift by  $-5 \text{ cm}^{-1}$  on average.<sup>[22]</sup> This is consistent with population of the carbonyl's antibonding  $\pi^*$  orbital presumably by overflow of the filled d<sup>10</sup> orbitals from the Cu<sup>I</sup> ion, via the tetrazine LUMO.<sup>[28]</sup>

The self-assembly of G<sup>+</sup> (Figure 2a) was shown by titration of the Cu<sup>I</sup> ion into a solution of ReB. Upon addition of 0.5 equivalents of Cu<sup>I</sup> to ReB, a single UV/Vis/NIR transition was observed to grow in at 752 nm (= 1.6 eV) with strong intensity ( $\epsilon = 8700 \text{ M}^{-1} \text{ cm}^{-1}$ ) and stable isosbestic points (Figure 2b), which is tentatively assigned to be MLCT in character. Equilibrium-restricted factor analysis<sup>[24]</sup> of the spectroscopic titration<sup>[22]</sup> is consistent with a self-assembly formation energy of  $\Delta G = -68 \text{ kJ mol}^{-1}$  for G<sup>+</sup>.

When the titration was repeated using CV (Figure 2c), a smooth change in the redox properties was observed. Upon addition of Cu<sup>I</sup>, the reduction of ReB centered at  $E' = -350 \text{ mV}$  decreased in intensity and three new redox couples grew in. These are observed at  $\approx 50\%$  peak intensity, which is attributed to the formation of G<sup>+</sup> at half the concentration of the initial ReB. The redox properties of G<sup>+</sup> are remarkable with the three redox processes attributed to each of the redox-active centers in G<sup>+</sup>: The Cu<sup>I</sup>/Cu<sup>II</sup> oxidation at +780 mV with the two couples at  $E' = +245$  and  $-270 \text{ mV}$  assigned to sequential one-electron reductions<sup>[26]</sup> of the first and second ReB moieties.

The large difference between the reduction potentials of the two coordinated ReB ligands (515 mV) is consistent with

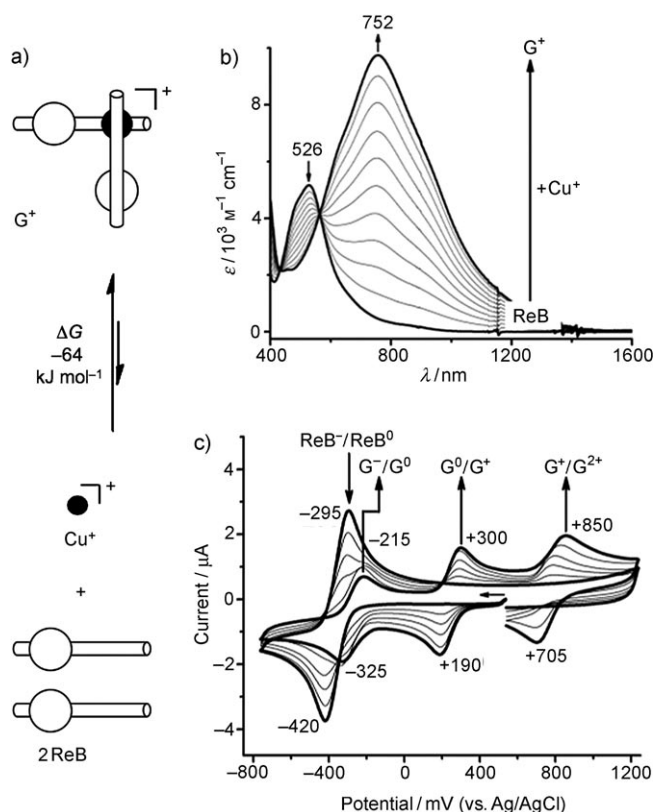


**Figure 2.** a) Self-assembly process for the formation of G<sup>+</sup> with  $\Delta G$  obtained from analysis of a UV/Vis/NIR titration recorded at 50  $\mu\text{M}$ . b) Titration of ReB with Cu<sup>+</sup> (CH<sub>2</sub>Cl<sub>2</sub>) recorded using UV/Vis/NIR spectroscopy ([ReB]<sub>0</sub> = 50  $\mu\text{M}$ , 0.5 equiv of Cu<sup>+</sup>) and c) CV ([ReB]<sub>0</sub> = 0.5 mM, 0.5 equiv of Cu<sup>+</sup>, 0.1 M TBAPF<sub>6</sub>, 0.2 V s<sup>-1</sup>, Ag/AgCl).

ligand mixed valency<sup>[20]</sup> where the metal acts as the bridge. This large peak separation corresponds to a comproportionation constant of  $K_c = 5.1 \times 10^8$ , indicating that there is an enhanced stabilization of the singly reduced species, [(ReB<sup>-</sup>)Cu(ReB)]<sup>0</sup>, by a strong electrochemical coupling between the ReB ligands when bridged by the Cu<sup>I</sup> ion. Presumably, this coupling is facilitated by the large LUMO coefficients on the tetrazine nitrogen atoms (ca. 25% on each)<sup>[17]</sup> and the small HOMO–LUMO gap. Consistently, strong coupling between the Cu<sup>I</sup> and ligand orbitals is implied by the breakdown in correspondence between the energy of the broad absorption band of G<sup>+</sup> at 752 nm and the potential difference from the Cu<sup>I</sup> oxidation to the first reduction ( $\Delta E_{\text{redox}} = 535 \text{ mV} \equiv 2300 \text{ nm}$ ). The large comproportionation constant cannot by itself distinguish between Class II, II/III or III mixed valency and further studies are ongoing.

Consistent with the unique electronic properties of G<sup>+</sup>, the carbonyl bands shift to higher energies<sup>[22]</sup> by +8 cm<sup>-1</sup> on average when compared to ReB. Therefore, the  $\pi$ -orbital manifold of the {Re(CO)<sub>3</sub>Cl} moieties are being depopulated by shifting electron density onto the tetrazine LUMO upon coordination of the Cu<sup>I</sup> ion in G<sup>+</sup>. We believe this can occur with the large energetic stabilization of the LUMO, as observed in the CV.

In the neutral state, [2]PR<sup>+</sup> is favored over G<sup>+</sup> by 5 kcal mol<sup>-1</sup>.<sup>[22]</sup> This situation was verified by a competition

experiment<sup>[22]</sup> where addition of the macrocycle, MC, to the grid corner, G<sup>+</sup>, led to the formation of the pseudorotaxane, [2]PR<sup>+</sup>, by ejecting one of the ReB ligands. Within this 1:1 mixture of [2]PR<sup>+</sup>:ReB, the reduction potentials of [2]PR<sup>+</sup> and G<sup>+</sup> and their corresponding stabilities indicate that redox-driven switching between the two architectures should be feasible.<sup>[22]</sup> A thermodynamic analysis indicated that the grid + macrocycle system is more stable than the pseudorotaxane mixture by -27 and -37 kJ mol<sup>-1</sup> for the mono and doubly reduced systems, respectively.

CVs of the self-sorting 1:1 mixture of [2]PR<sup>+</sup>:ReB were observed to change reversibly as a function of scan rate.<sup>[22]</sup> Such changes are a hallmark for redox-induced switching.<sup>[29]</sup> For demonstration purposes, the CVs were recorded (Figure 3) at a fast scan rate (20 V s<sup>-1</sup>) to provide a snap

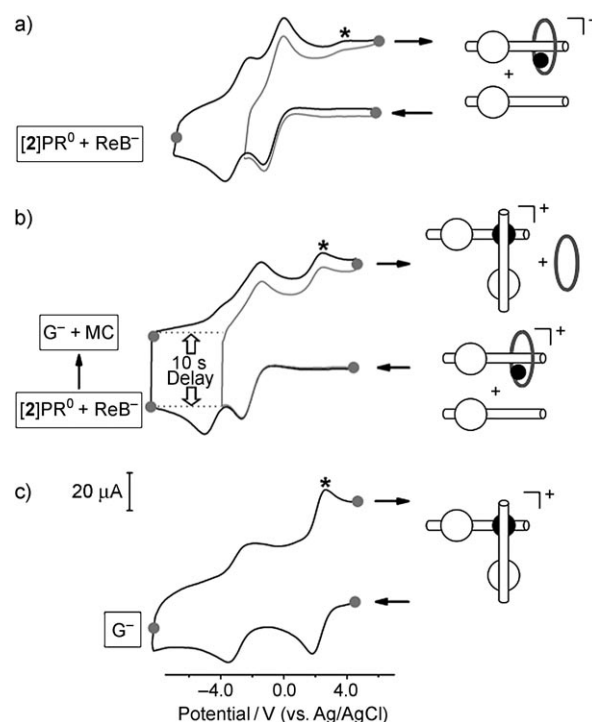


**Figure 3.** Annotated CV experiments (20 V s<sup>-1</sup>, iR compensated) of a) a 1:1 molar ratio of ReB:[2]PR<sup>+</sup> b) a 1:1 molar ratio of ReB:[2]PR<sup>+</sup> recorded with a vertex delay of 10 s to allow time for molecular switching to occur, and c) isolated G<sup>+</sup> recorded to pinpoint peak positions (ca. 0.5 mM, 0.1 M TBAPF<sub>6</sub>, CH<sub>2</sub>Cl<sub>2</sub>, Ag/AgCl).

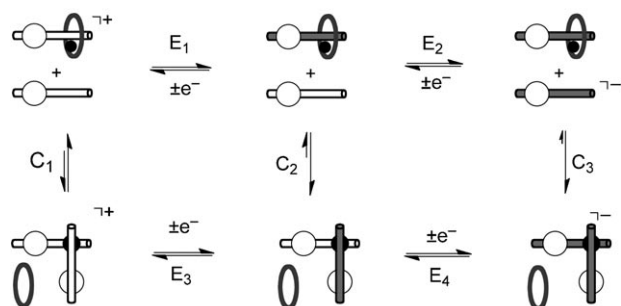
shot of the solution composition.<sup>[25a]</sup> Starting from the equimolar mixture of ReB and [2]PR<sup>+</sup>, the CV shows (Figure 3a) two cathodic peaks in the forward scan, as expected for the reduction of two species in solution, [2]PR<sup>+</sup> at  $E' = -125 \text{ mV}$  and ReB at  $E' = -350 \text{ mV}$ , and their corresponding anodic peaks in the reverse scan. In a second CV experiment (Figure 3b), a vertex delay time of 10 s was introduced at the end of the first linear sweep<sup>[25b]</sup> to allow time for the switching to take place. Therefore, at the end of the forward sweep (-0.7 V), the reduced forms of the original species are present, i.e., ([2]PR<sup>0</sup> + ReB<sup>-</sup>). Pausing here for 10 s allows the mixture to re-sort from the original [2]pseu-



dorotaxane architecture, i.e.,  $[(\text{ReB}^-)\text{Cu}^+(\text{MC})]^0$ , into the doubly reduced homoleptic grid-corner complex  $\text{G}^-$ , i.e.,  $[(\text{ReB}^-)\text{Cu}^+(\text{ReB}^-)]^-$ , by incorporating  $\text{ReB}^-$  and ejecting MC. Consistent with this picture, the return sweep of the CV shows two anodic peaks at the locations corresponding to  $\text{G}^+$  (Figure 3c).<sup>[30]</sup> The diagnostic feature for formation of  $\text{G}^-$  is the anodic peak at +400 mV (marked with an asterisk, \*).

Interestingly, the grid architecture,  $\text{G}^-$ , could also be accessed by pausing the CV at an intermediate potential (−0.3 V) that can reduce  $[2]\text{PR}^+$  but not  $\text{ReB}$ . Without the delay (Figure 3a, gray line) there is insufficient time (20 ms) for switching and only one redox peak was observed in the return sweep consistent with retention of  $[2]\text{PR}^0$ . With a 10 s delay (Figure 3b, gray line), the reverse sweep shows two redox peaks readily assigned to the homoleptic grid corner,  $\text{G}^-$ . In this case, reduced  $[2]\text{PR}^0$  and neutral  $\text{ReB}^0$  can re-sort into the mixed-valent state of the homoleptic complex  $\text{G}^0$ , that is,  $[(\text{ReB}^-)\text{Cu}^+(\text{ReB})]^0$ . Thus a large amount of the driving force (−27 kJ mol<sup>−1</sup>) for this switching stems from the additional stabilization that the electron enjoys in the mixed-valent state of the grid corner. Such mixed-valent stabilization of a supramolecular complex is rare but not unprecedented.<sup>[31]</sup> The applied potential (−0.3 V) is more negative than that required to doubly reduce the homoleptic complex, thus, potential inversion causes facile reduction to  $\text{G}^-$ .

The entire switching process can be represented as an extended square scheme (Scheme 2) where the electrochemical (E) processes are represented along the horizontal axis and



**Scheme 2.** Extended square scheme representing the chemical (C) and electrochemical (E) steps in the switching process. White and gray units represent neutral and reduced  $\text{ReB}$ , respectively.

the chemical processes along the vertical axis. The two scan windows used in the CV studies show that two different pathways can be followed for switching in the forwards direction: An  $\text{E}_1\text{E}_2\text{C}_3$  sequence operates when both starting components are reduced at −0.7 V and an  $\text{E}_1\text{C}_2\text{E}_4$  sequence when only the first component is initially reduced at −0.3 V. Both generate  $\text{G}^-$ , and the return process again follows two different pathways depending upon the potential. An  $\text{E}_4\text{C}_2\text{E}_1$  pathway is followed when  $\text{G}^-$  is monooxidized at −0.2 V to its mixed-valent state and an  $\text{E}_4\text{E}_3\text{C}_1$  pathway when  $\text{G}^-$  is fully reoxidized back to  $\text{G}^+$  at +0.6 V.<sup>[22]</sup>

The switching mechanism was investigated using digital CV simulations.<sup>[14]</sup> The reorganization from both the singly and doubly reduced mixtures into the grid corner occurs

through bimolecular pathways as verified by variable-concentration CVs.<sup>[22,32]</sup> For equilibria  $\text{C}_2$  and  $\text{C}_3$  (Scheme 2), the associated rate constants are  $k_2^{298} = 1 \times 10^4$  and  $5 \times 10^4 \text{ M}^{-1} \text{ s}^{-1}$ , respectively. Association-activated processes are consistent with patterns of ligand exchange around  $\text{Cu}^I$  ions.<sup>[13]</sup> These rate constants are similar to those seen for related  $\text{Cu}^I$  pseudorotaxanes.<sup>[14]</sup> We believe that in our system the vacant chelating site on  $\text{ReB}$  associates with  $\text{Cu}^I$  concerted with the loss of MC. The reverse switching process was too fast (> 15 ms), even at 258 K, to analyze the mechanism.<sup>[22]</sup>

Received: February 17, 2010

Published online: May 20, 2010

**Keywords:** mixed-valent compounds · molecular architectures · molecular switches · self-assembly

- a) J. M. Lehn, *Science* **2002**, 295, 2400–2403; b) J. R. Nitschke, *Acc. Chem. Res.* **2007**, 40, 103–112.
- M. Fujita, *Chem. Soc. Rev.* **1998**, 27, 417–425.
- S. R. Seidel, P. J. Stang, *Acc. Chem. Res.* **2002**, 35, 972–983.
- E. R. Kay, D. A. Leigh, F. Zerbetto, *Angew. Chem.* **2007**, 119, 72–196; *Angew. Chem. Int. Ed.* **2007**, 46, 72–191.
- a) R. A. Bissell, E. Cordova, A. E. Kaifer, J. F. Stoddart, *Nature* **1994**, 369, 133–137; b) D. J. Cardenas, A. Livoreil, J.-P. Sauvage, *J. Am. Chem. Soc.* **1996**, 118, 11980–11981.
- A. Mirzoian, A. E. Kaifer, *Chem. Eur. J.* **1997**, 3, 1052–1058.
- A. Credi, S. Dumas, S. Silvi, M. Venturi, A. Arduini, A. Pochini, A. Secchi, *J. Org. Chem.* **2004**, 69, 5881–5887.
- P. Mal, D. Schultz, K. Beyeh, K. Rissanen, J. R. Nitschke, *Angew. Chem.* **2008**, 120, 8421–8425; *Angew. Chem. Int. Ed.* **2008**, 47, 8297–8301.
- H. Y. Zhang, Q. C. Wang, M. H. Liu, X. Ma, H. Tian, *Org. Lett.* **2009**, 11, 3234–3237.
- J. Ramirez, A. M. Stadler, N. Kyritsakas, J. M. Lehn, *Chem. Commun.* **2007**, 237–239.
- S. Hiraoka, Y. Sakata, M. Shionoya, *J. Am. Chem. Soc.* **2008**, 130, 10058–10059.
- P. J. Lusby, P. Muller, S. J. Pike, A. M. Z. Slawin, *J. Am. Chem. Soc.* **2009**, 131, 16398–16400.
- a) U. M. Frei, G. Geier, *Inorg. Chem.* **1992**, 31, 187–190; b) U. M. Frei, G. Geier, *Inorg. Chem.* **1992**, 31, 3132–3137.
- a) K. A. McNitt, K. Parimal, A. I. Share, A. C. Fahrenbach, E. H. Witlicki, M. Pink, D. K. Bediako, C. L. Plaisier, N. Le, L. P. Heeringa, D. A. Vander Griend, A. H. Flood, *J. Am. Chem. Soc.* **2009**, 131, 1305–1313; b) A. I. Share, K. Parimal, A. H. Flood, *J. Am. Chem. Soc.* **2010**, 132, 1665–1675.
- K. Mahata, M. Schmittel, *J. Am. Chem. Soc.* **2009**, 131, 16544–16554.
- S. D. Ernst, W. Kaim, *Inorg. Chem.* **1989**, 28, 1520–1528.
- G. F. Li, K. Parimal, S. Vyas, C. M. Hadad, A. H. Flood, K. D. Glusac, *J. Am. Chem. Soc.* **2009**, 131, 11656–11657.
- M. Meyer, A. M. Albrecht-Gary, C. O. Dietrich-Buchecker, J.-P. Sauvage, *Inorg. Chem.* **1999**, 38, 2279–2287.
- E. L. Rosen, C. D. Varnado, A. G. Tennyson, D. M. Khranov, J. W. Kamplain, D. H. Sung, P. T. Cresswell, V. M. Lynch, C. W. Bielawski, *Organometallics* **2009**, 28, 6695–6706.
- Y. Sasaki, M. Abe, *Chem. Rec.* **2004**, 4, 279–290.
- G. J. Kubas, B. Monzyk, A. L. Crumbliss, *Inorg. Synth.* **1990**, 28, 68–70.
- See the Supporting Information.
- T. Scheiring, J. Fiedler, W. Kaim, *Organometallics* **2001**, 20, 1437–1441.

- [24] D. A. Vander Griend, D. K. Bediako, M. J. DeVries, N. A. DeJong, L. P. Heeringa, *Inorg. Chem.* **2008**, *47*, 656–662.
- [25] a) A linear scan from +0.5 to –0.8 V at 20 V s<sup>–1</sup> takes 65 ms. b) The time available for switching can be estimated from the position of the redox peaks that start and stop switching. For the simplest case (Figure 3b), the potential scanned from [2]PR<sup>+</sup> reduction to its reoxidation (0.4 V) is equal to 20 ms. This time is extended by 10 s with the delay.
- [26] All redox processes are assigned to the transfer of one electron on the basis of prior coulometry (Ref. [14a]) and similar systems (Ref. [16]), as well as by comparison to the one-electron Cu<sup>I</sup>/Cu<sup>II</sup> oxidation.
- [27] Some of the large peak separations in the CVs stem from slow electron-transfer kinetics as noted in the Supporting Information.
- [28] G. J. Stor, F. Hartl, J. W. M. Vanoutersterp, D. J. Stufkens, *Organometallics* **1995**, *14*, 1115–1131.
- [29] A. Kaifer, M. Gómez-Kaifer, *Supramolecular Electrochemistry*, Wiley-VCH, Weinheim, **2007**.
- [30] The reverse sweep in Figure 3b shows a small remnant signature of ReB and [2]PR<sup>+</sup>, which alters the shape of the CV. These species reflects the non-equilibrium nature at the electrode–solution interface.
- [31] a) J. C. Curtis, J. A. Roberts, R. L. Blackburn, Y. Dong, M. Massum, C. S. Johnson, J. T. Hupp, *Inorg. Chem.* **1991**, *30*, 3856–3860; b) K. T. Potts, M. Keshavarz-K, F. S. Tham, K. A. Gheysen Raiford, C. Arana, H. D. Abruña, *Inorg. Chem.* **1993**, *32*, 5477–5484; c) M. Yoshizawa, K. Kumazawa, M. Fujita, *J. Am. Chem. Soc.* **2005**, *127*, 13456–13457; d) B. J. Lear, C. P. Kubiak, *J. Phys. Chem. B* **2007**, *111*, 6766–6771; e) P.-T. Chiang, N.-C. Chen, C.-C. Lai, S.-H. Chiu, *Chem. Eur. J.* **2008**, *14*, 6546–6552.
- [32] CV simulations for a dissociative pathway generated thermodynamic and kinetic constants that were not physically meaningful.